第40回ネットワーク科学勉強会参加者のみ閲覧可。
二次配布はご遠慮下さい。

第40回ネットワーク科学勉強会（2025年4月24日）

Multi-scale Laplacian community detection in heterogeneous networks

Pablo Villegas, Andrea Gabrielli*, Anna Poggialini & Tommaso Gili

Physical Review Research 7, 013065 (2025)

報告：岡本 洋（東京大学）

Summary

- Finding multi-scale mesoscopic organization of communities is still a fundamental and open problem in complex network theory.
- Leveraging the **Laplacian Renormalization Group (LRG)**, we analyze information diffusion pathways across networks to shed light on this issue.

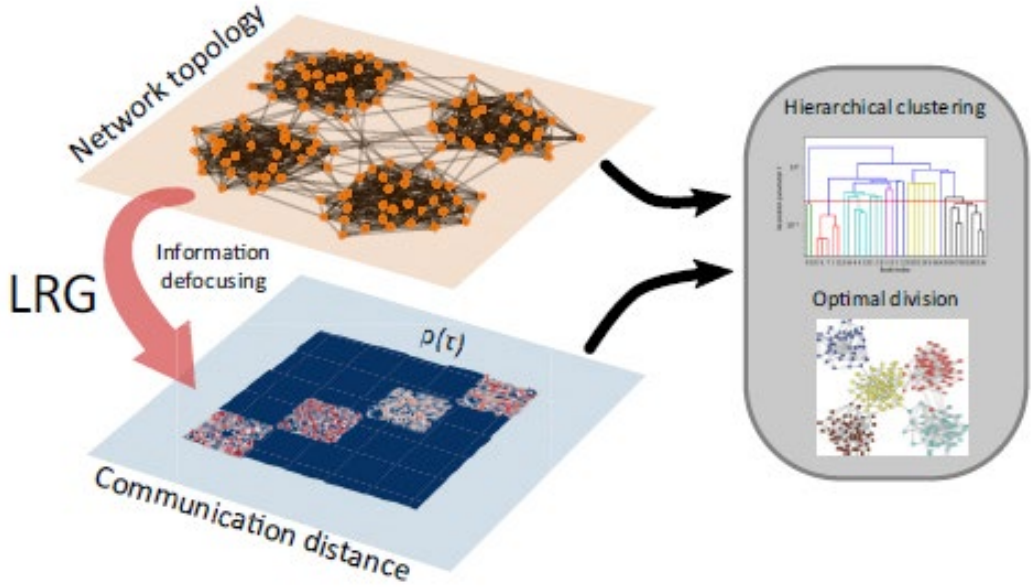

FIG. 1. Defining multiscale Kadanoff supernodes. *Communication distance* between nodes reflects the underlying hidden complex topology, capturing the internodes communicability and giving a natural merging of nodes at specific times τ. The LRG gives a natural interpretation of the network scales in terms of network eigenmodes, thereby enabling a deeper understanding of the mesoscopic properties of the network.

Related publications by the authors:

- P. Villegas, A. Gabrielli, F. Santucci, G. Caldarelli, T. Gili. Laplacian paths in complex networks: Information core emerges from entropic transitions, *Physical Review Research* 4, 033196 (2022). [33]
- P. Villegas, T. Gili, G. Caldarelli, A. Gabrielli. Laplacian renormalization group for heterogeneous networks. *Nature Physics* 19, 445 (2023). [17]
- A. Poggialini, P. Villegas, M. A. Muñoz, A. Gabrielli. Networks with Many Structural Scales: A Renormalization Group Perspective. *Physical Review Letters* 134, 057401 (2025).

Real-space renormalization group (RG)

Consider a Hamiltonian $\mathcal{H}\big(\sigma(x)\big)$.

(e.g. $\sigma(x)$ represents the field of local mean spin at a real-space point x.)

The key concept of the RG is to find an effective Hamiltonian at scale λ, $\mathcal{H}(\sigma) \rightarrow \mathcal{H}_{\lambda}(\sigma)$.

Real-space renormalization group (RG)

The procedure of RG (Kadanoff blocks (1966)):

1. Gorup the lattice points into blocks of b^2 ones.
2. Replace each block with a single point of size b following some rule $\mathcal{R}_g(\sigma)$, e.g. the majority rule.
3. Rescale by a factor b to return to the original lattice spacing a.

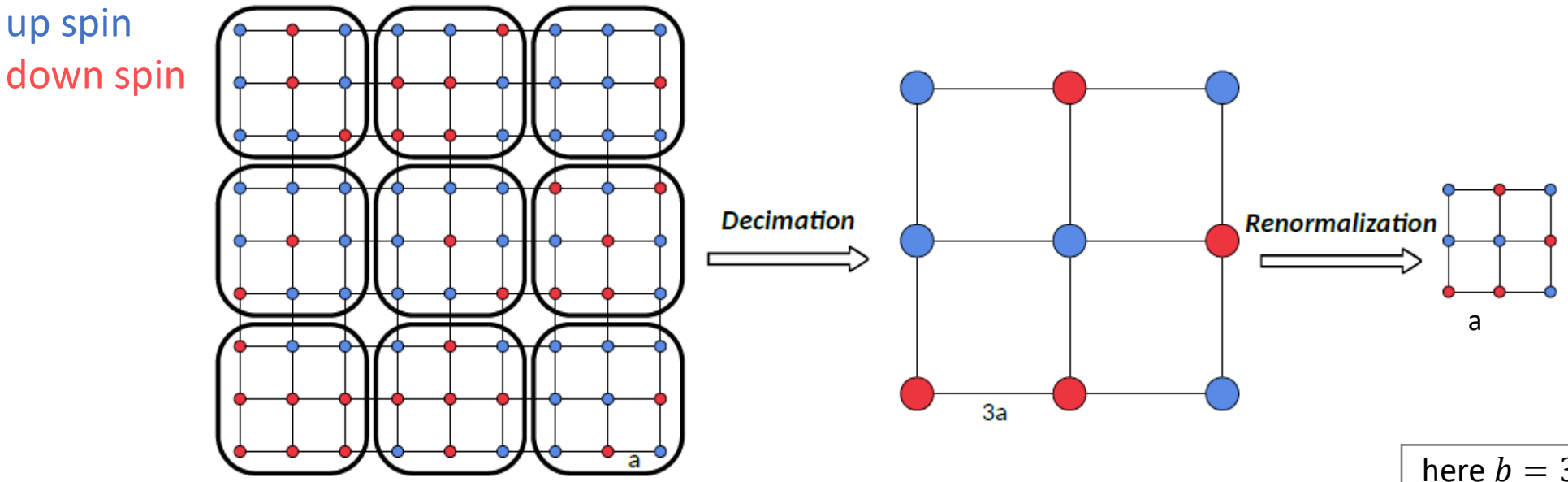

FIG. 1: Sketch the decimation process employing Kadanoff blocks on a square lattice of side a, where blue (red) points represent up (down) spins, respectively. The lattice is divided into several blocks with b^2 sites which are now coarse-grained, replacing it with a single-block following some rule $\mathcal{R}_g(\sigma)$, finally reducing all the system scales by a factor b. This scheme produces a reduced version of the original system.

Supplementally Information of [17]

Real-space renormalization group (RG)

Application of the Kadanoff blocks to the Ising model

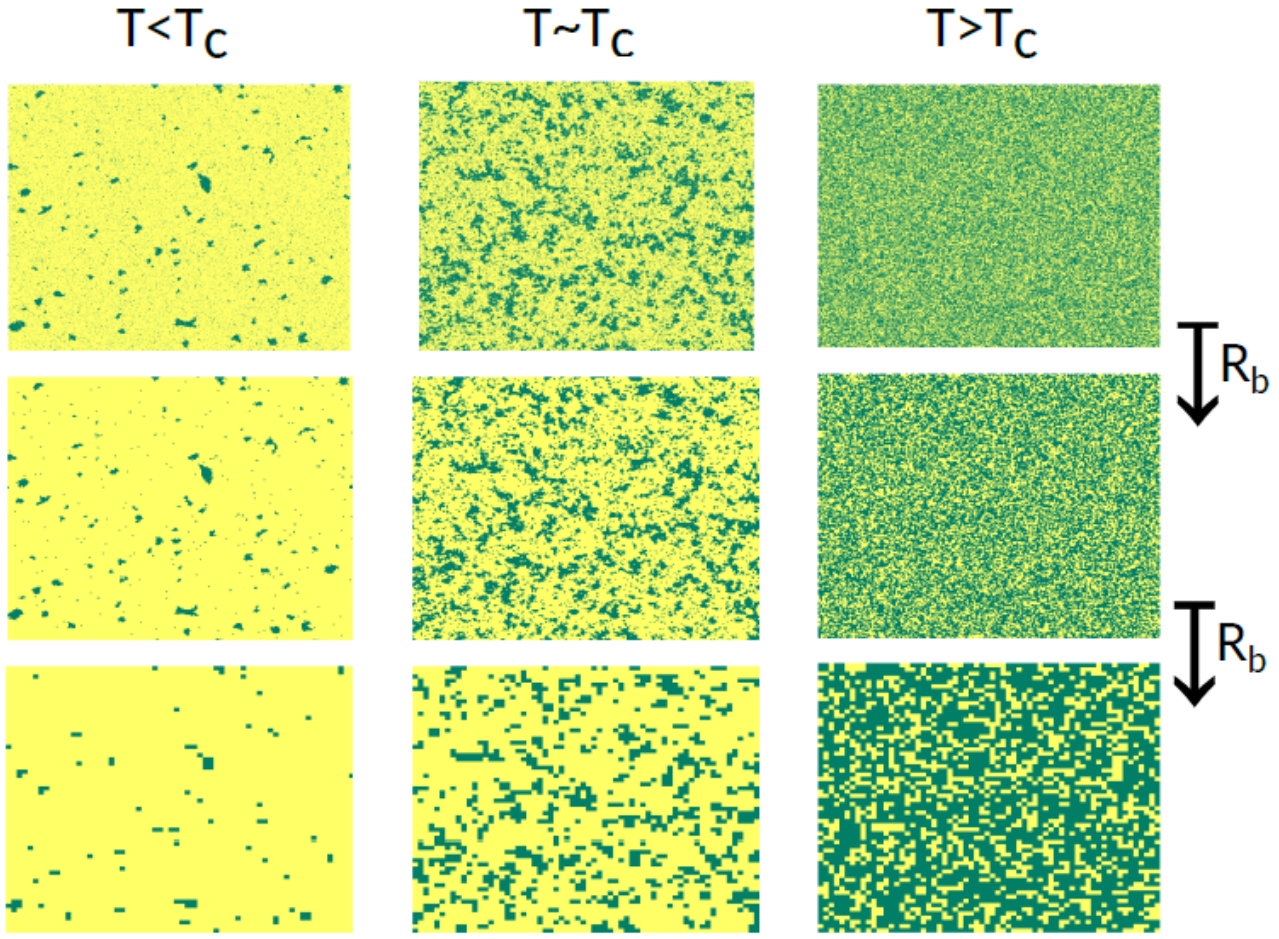

FIG. 2: (a) RG process for the Ising model simulated in a 2D lattice of $L = 1024$ (upper panels), and employing Kadanoff blocks of size $b = 3$. The three panels correspond to different temperatures $T < T_c$, $T \sim T_c$, and $T > T_c$, respectively. The RG process is performed from top to bottom scales of the figure, revealing the RG flow of the dynamical process.

Supplementally Information of [17]


高橋和孝・西森秀稔 共著
相転移・臨界現象とくりこみ群
丸善出版

Graph Laplacian $\mathbf{L} = \mathbf{I} - \mathbf{A}$

1次元空間上の拡散

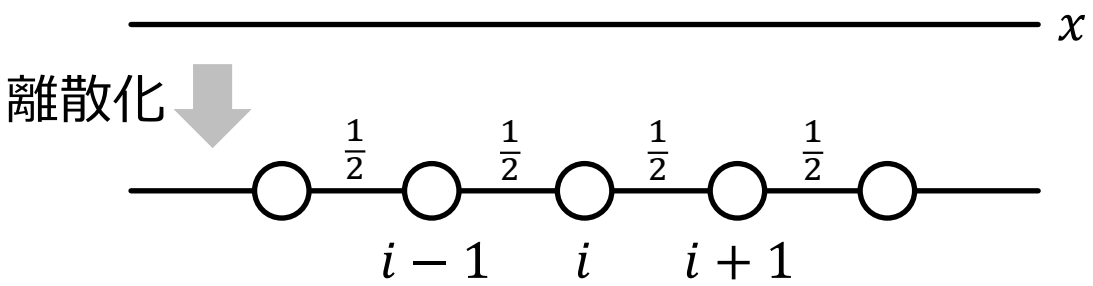

拡散方程式：

$$\frac{\partial \phi(x,t)}{\partial t} = D\nabla^2 \phi(x,t) = D\frac{\partial^2 \phi(x,t)}{\partial x^2}$$

∇^2 : Laplacian operator

離散化：

$$\frac{d\phi_i(t)}{dt} = D\left[\phi_{i+1}(t) - 2\phi_i(t) + \phi_{i-1}(t)\right] = -2D\left[\phi_i(t) - \frac{1}{2}\phi_{i+1}(t) - \frac{1}{2}\phi_{i-1}(t)\right]$$

ベクトル標記 $\left(\vec{\phi}(t) = \left(\cdots, \phi_{i-1}(t), \phi_i(t), \phi_{i+1}, \cdots\right)^\top\right)$:

$$\frac{d}{dt}\vec{\phi}(t) = -2D\left[\mathbf{I} - \mathbf{A}\right]\vec{\phi}(t)$$

$$\mathbf{I} = \begin{pmatrix} 1 & 0 & 0 & 0 & 0 \\ 0 & \ddots & 0 & 0 & 0 \\ 0 & 0 & 1 & 0 & 0 \\ 0 & 0 & 0 & \ddots & 0 \\ 0 & 0 & 0 & 0 & 1 \end{pmatrix}, \quad \mathbf{A} = \begin{pmatrix} \ddots & 1/2 & 0 & 0 & 0 \\ 1/2 & 0 & 1/2 & 0 & 0 \\ 0 & 1/2 & 0 & 1/2 & 0 \\ 0 & 0 & 1/2 & 0 & 0 \\ 0 & 0 & 0 & 1/2 & \ddots \end{pmatrix}$$

Graph Laplacian :

$\mathbf{L} \triangleq \mathbf{I} - \mathbf{A}$

ネットワーク上の拡散

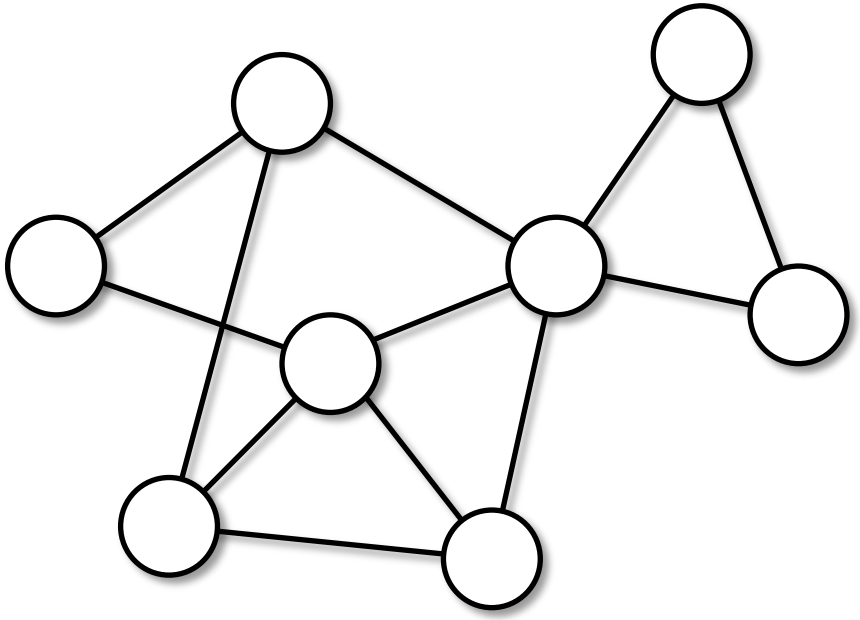

$$\frac{d}{dt}\mathbf{s}(t) = -\mathbf{L}\mathbf{s}(t)$$

$$\mathbf{L} \triangleq \mathbf{I} - \mathbf{A}$$

I. Statistical physics of information network diffusion

Adjacency matrix of the network:

$\hat{A} = [A_{ij}]$. (Assume undirected: $A_{ij} = A_{ji}$.)

Laplacian:

$\hat{L} = [L_{ij}] = [\delta_{ij} \sum_k A_{ik} - A_{ij}]$.

Time evolution of the network state $\boldsymbol{s}(t)$:

$\dot{\boldsymbol{s}}(t) = -\hat{L}\boldsymbol{s}(t)$.

Formal solution:

$\boldsymbol{s}(\tau) = e^{-\tau\hat{\boldsymbol{L}}}\boldsymbol{s}(0)$.

Propagator:

$\widehat{K}(\tau) = e^{-\tau\hat{\boldsymbol{L}}}$

I. Statistical physics of information network diffusion

Define the ensemble of accessible information:

$$\hat{\rho}(\tau) = \frac{\widehat{K}(\tau)}{\mathrm{Tr}\left(\widehat{K}(\tau)\right)} = \frac{e^{-\tau\hat{L}}}{\mathrm{Tr}\left(e^{-\tau\hat{L}}\right)},$$

which is the **density matrix** in statistical physics ($\hat{L}$ Hamiltonian and τ inverse temperature).

$$\mathrm{Tr}\left(e^{-\tau\hat{L}}\right) = \sum_{i=1}^{N} e^{-\tau\lambda_i},$$

where λ_i are the eigenvalues of $\hat{L}$.

One can therefore define the network **entropy**:

$$S[\hat{\rho}(\tau)] = -\mathrm{Tr}[\hat{\rho}(\tau)\log_{10}\hat{\rho}(\tau)] = -\frac{1}{\log_{10} N}\sum_{i=1}^{N} \nu_i(\tau)\log_{10}\nu_i(\tau),$$

where ν_i are the eigenvalues of $\hat{\rho}(\tau)$ (i.e., $\nu_i(\tau) = e^{-\tau\lambda_i}$).

[34] M. De Domenico, J. Biamonte. Phys. Rev. X (2016)
[35] A. Ghavasieh, C. Nicolini, M. De Domenico, Phys. Rev. E (2020)

I. Statistical physics of information network diffusion

The specific heat, defined by the derivative of the entropy with respect to τ

$$C(\tau) = -\frac{dS}{d\log_{10}\tau},$$

is a detector of structural transition points.

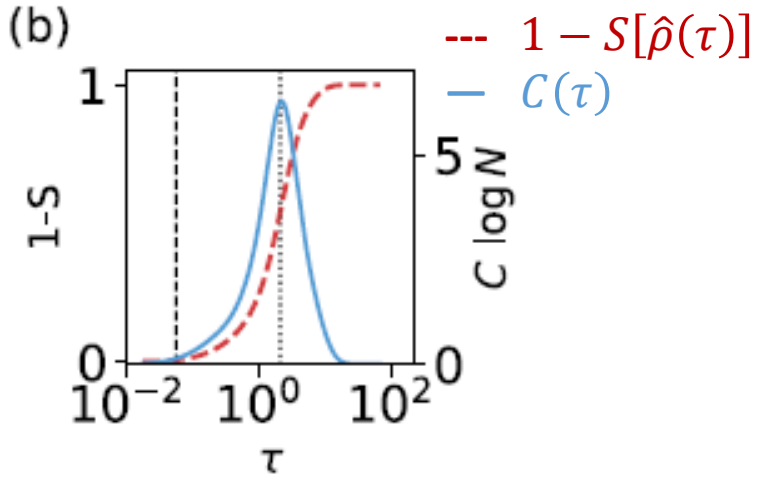

II. Laplacian renormalization group (LRG)

How to implement the RG theory for complex networks that lack a well-defined special embedding?

Fourier-space (eigenvector-space) version of Kadanoff scheme (KG Wilson 1974)

The Laplacian operator $\hat{L}$, as symmetric and real-valued, has a complete set of N eigenvectors $\{|\lambda\rangle\}$ with semipositive eigenvalues $\{\lambda\}$.

Hence $\hat{L}$ is decomposed as

$$\hat{L} = \sum_i \lambda_i |\lambda_i\rangle\langle\lambda_i| = \sum_\lambda \lambda |\lambda\rangle\langle\lambda| \, .$$

The $1/\lambda_i$ represents the time scale of the i-th eigenmode.

Thus, $\hat{L}$ contains multiple time scales characterising the network diffusion.

II. Laplacian renormalization group (LRG)

The LRG step consists of integrating out faster eigenmodes from the Laplacian and rescaling the network, which correspond to Kadanoff blocks.

1. Reduce the Laplacian operator to the contribution of the $N - n$ slower eigenmodes:

   $\tilde{\hat{L}} = \sum_{\lambda<\tilde{\lambda}} \lambda|\lambda\rangle\langle\lambda|$.

2. Then rescale the time $\tau \to \tau'' = \tau/\tilde{\tau}$, so that $\tilde{\tau} = 1/\tilde{\lambda}$ in τ becomes the unit interval in τ''.

3. Redefine the coarse-grained Laplacian:

   $\hat{L}'' = \tilde{\tau}\tilde{\hat{L}}$.

II. Laplacian renormalization group (LRG)

LRG transformation for a BA network ($N = 512, m = 1$)

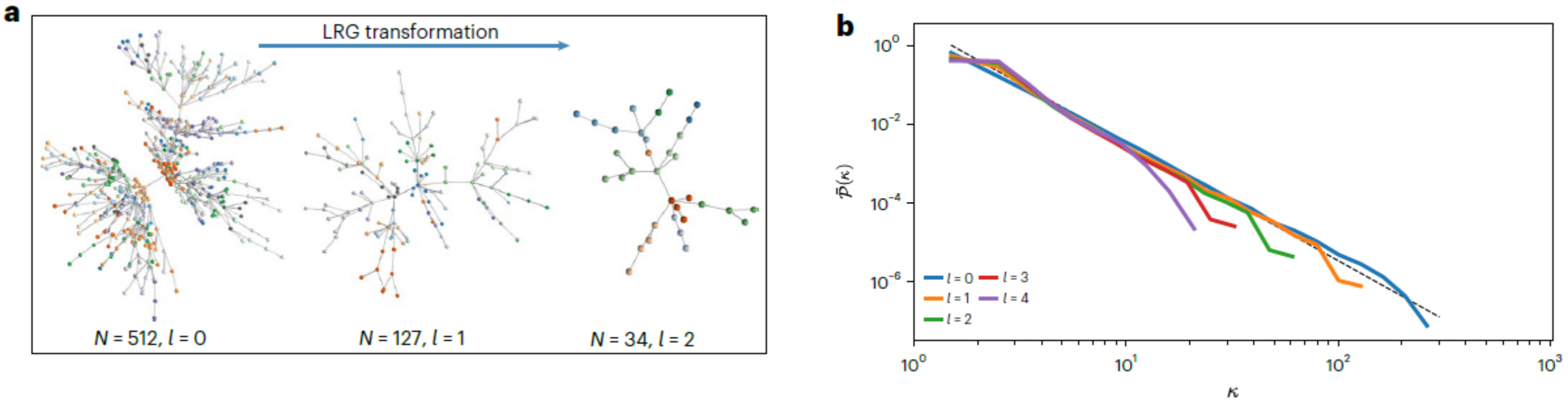

From **Fig.3** of [17] Villegas, P. et al. *Nature Physics* 19, 445-450 (2023)

III. Communication distance

The operator $\widehat{K}(\tau) = e^{-\tau\hat{L}}$ accounts for the sum of diffusion trajectories along all possible paths connecting nodes i and j.

Therefore, $\widehat{K}(\tau)$ (or equivalently $\hat{\rho}(\tau)$) gives a measure of information communicability between any pair of nodes at time scale τ.

Therefore, we define a **communicability distance** between noes i and j as

$\mathcal{D}_{ij}(\tau) = \left(1 - \delta_{ij}\right)/K_{ij}(\tau)$ (or equivalently $\mathcal{D}_{ij}(\tau) = \left(1 - \delta_{ij}\right)/\rho_{ij}(\tau)$).

The larger $\mathcal{D}_{ij}(\tau)$, the less the communicability on a time τ between nodes i and j.

IV. Community detection

$\mathcal{D}_{ij}(\tau)$ allows to use conventional algorithms in a metric space to solve clustering problems.

Here we choose the **Ward method**, which solves clustering (community detection) problems constructing dendrograms:

- Merge two clusters if the mean distance $\overline{\mathcal{D}}$ between any node in the first cluster and any node in the second cluster becomes smaller than the chosen threshold Δ.
- The output of this algorithm is a hierarchical tree (without null-model assumption).
- Note that **different dendrograms are obtained for different τ**.

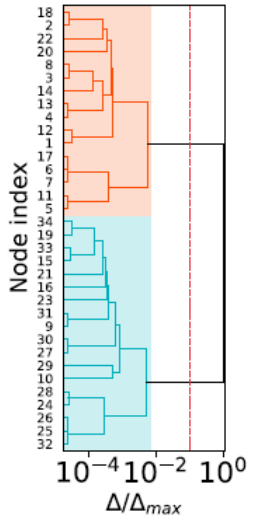

IV. Community detection

We propose a standard for selecting the **optimal cut** in every dendrogram **at a fixed τ**.

- Define the partition stability index:

  $$\Psi(n;\tau) = \mathcal{N}\left[\log_{10}\Delta_n(\tau) - \log_{10}\Delta_{n+1}(\tau)\right],$$

  where $\Delta_n(\tau)$ is the threshold Δ corresponding to the n-th dendrogram branching; $\mathcal{N} = \left[\log_{10}\Delta_1(\tau) - \log_{10}\Delta_{n_{max}}(\tau)\right]^{-1}$ is a normalization constant.

- Select the optimal cut of the dendrogram at n maximizing $\Psi(n;\tau)$. (Though, $\Psi(n;\tau)$ can present multiple local maxima.)

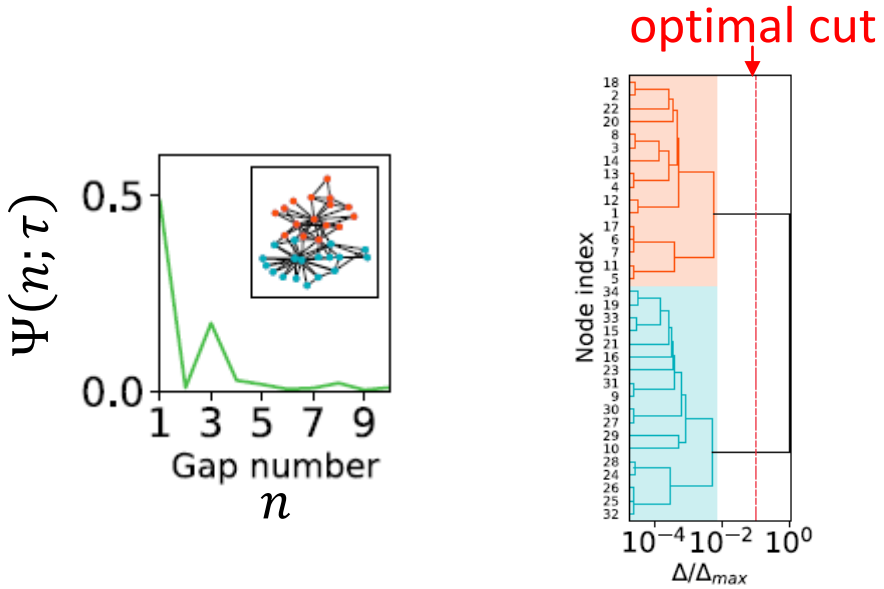

Fig. 2: Zachary's karate club

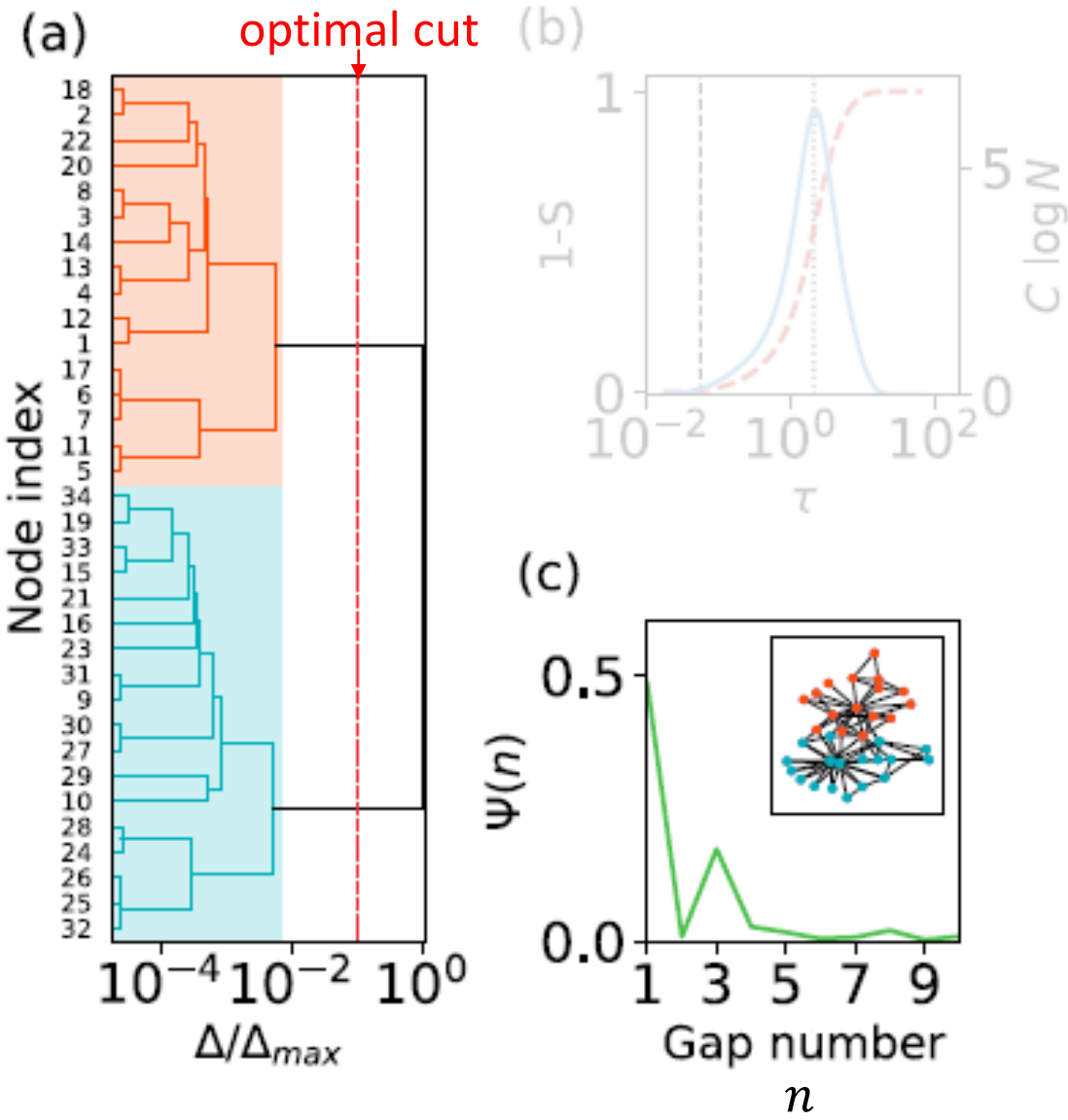

FIG. 2. LRG multiscale decomposition. (a) Normalized dendrogram for the Zachary's karate club with $\tau \lesssim \tau' = 1/\lambda_{\max}$. The red dashed line reflects the optimal division as stated by the maximum of Ψ. Different communities are shaded in different colors. (b) Entropy parameter [red dashed line, $(1 - S)$] and specific heat (blue solid line, C) versus the temporal resolution parameter of the network, τ. Black dashed line indicates $\tau' = 1/\lambda_{\max}$. The black dotted line indicates the time of the maximum heat capacity, τ^*. (c) Partition stability index Ψ versus gap number for $\tau \lesssim \tau'$. Note the high Ψ values giving place to the usual division in two and four communities of Zachary's karate club. Inset shows optimal division into communities of the network.

IV. Relevance to LRG

The LRG is relevant in the context that, by varying τ, the density operator $\hat{\rho}$ acts as a scanner of the characteristic network scales.

Starting from the smallest network scale $\tau' \sim 1/\lambda_{\max}$, one can consider progressively larger diffusion times integrating out smaller eigenmodes up to $\tau \sim 1/\lambda_{\text{gap}}$, where λ_{gap} is the second smallest (i.e. positive smallest) eigenvalue (Fiedler eigenvalue).

Meanwhile. the characteristic time scale of the network, τ^*, can be detected by the peak of the susceptibility (i.e. specific heat) $C(\tau) = -dS/d\log_{10}\tau$.

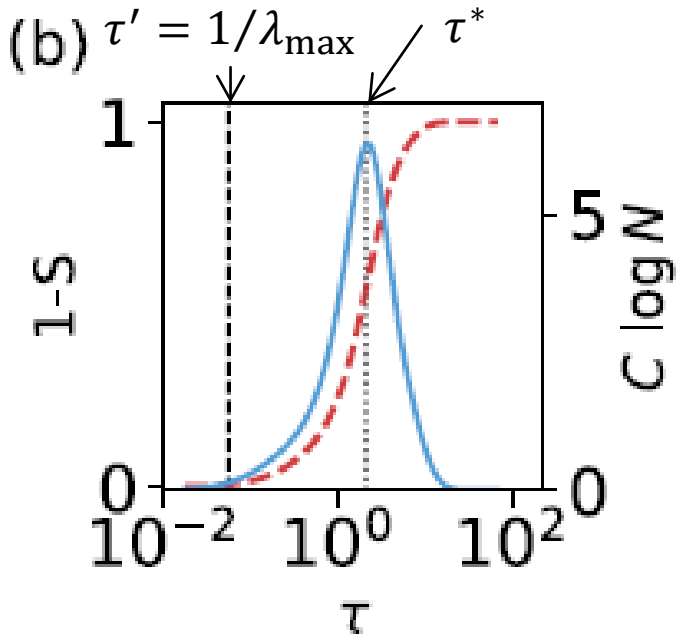

Tips

Existence of metastable nodes that switch groups to which they belong at different scales.

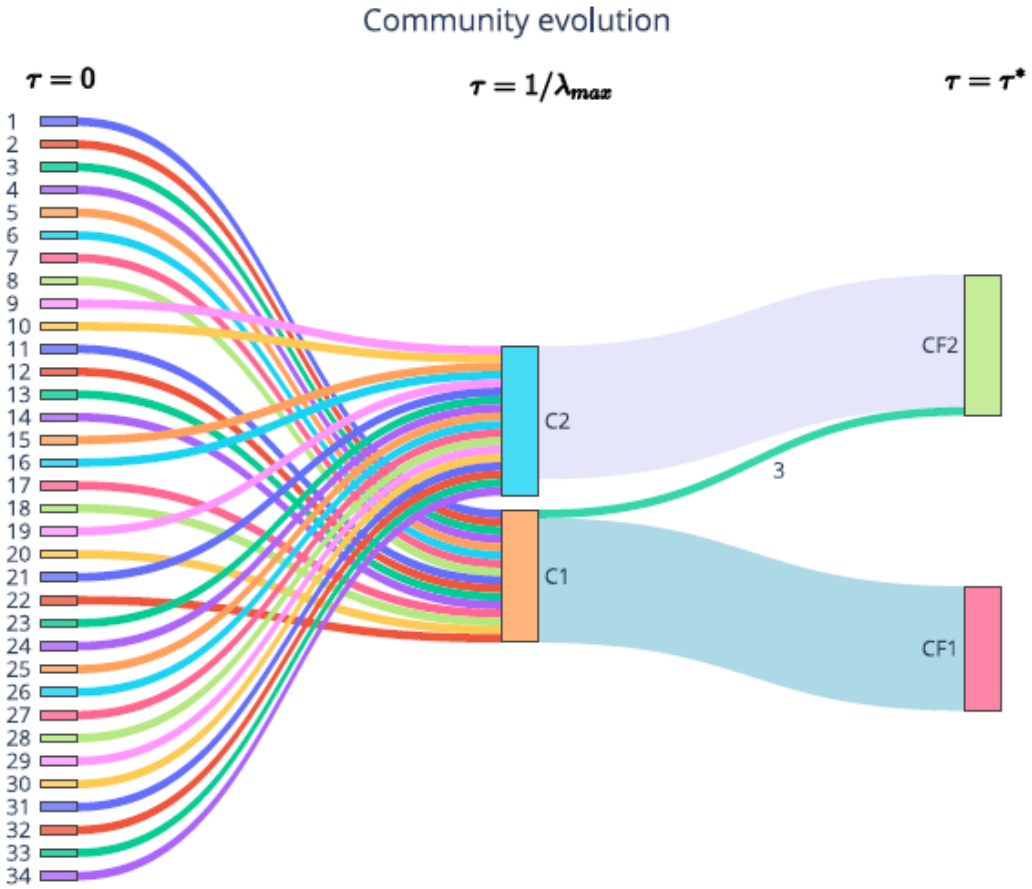

FIG. 5. Sankey diagram. Evolution of the optimal community division (in terms of Ψ) for Zachary's karate club at three different characteristic times. We emphasize the ability of "bridge nodes" to dynamically change their functional community at different timescales. We estimate the characteristic time of change of Node 3 at $\tau = 0.29(1) \simeq 5.26\tau'$.

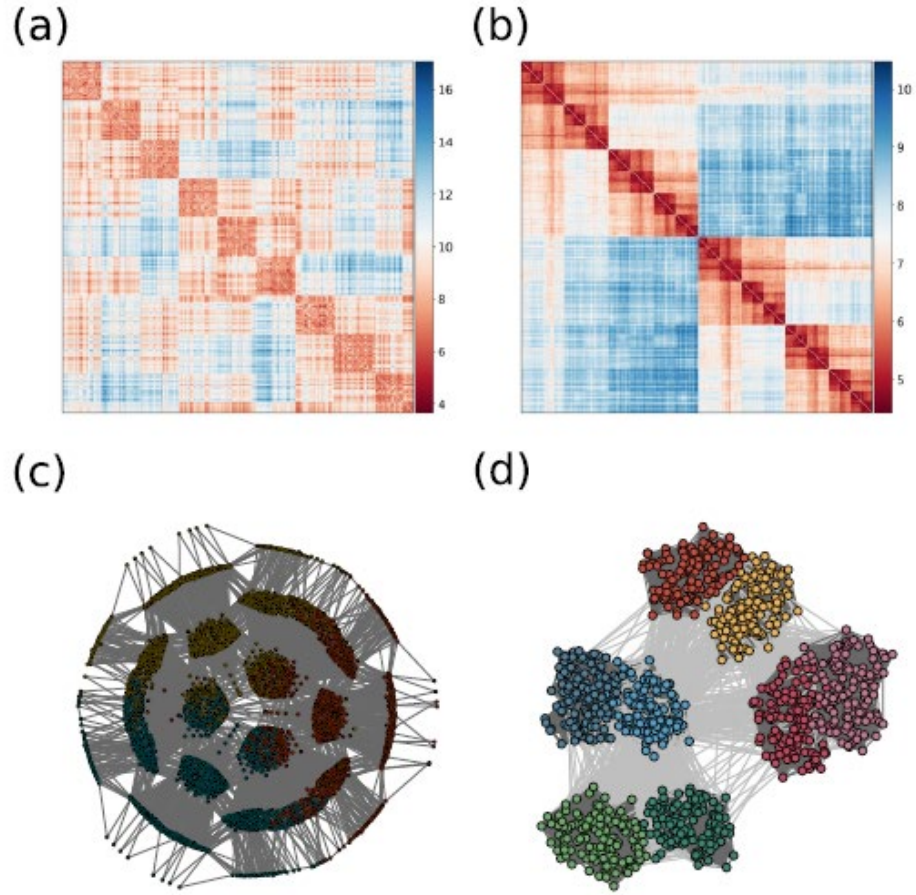

FIG. 3. Nested structures. Logarithm of the communication distance at $\tau' = 1/\lambda_{\max}$ for (a) a DGM graph, and (b) a hierarchic modular network with core-periphery structure (HM-CP). (c) Division into three communities for the DGM case and (d) division into eight communities for a HM-CP network.

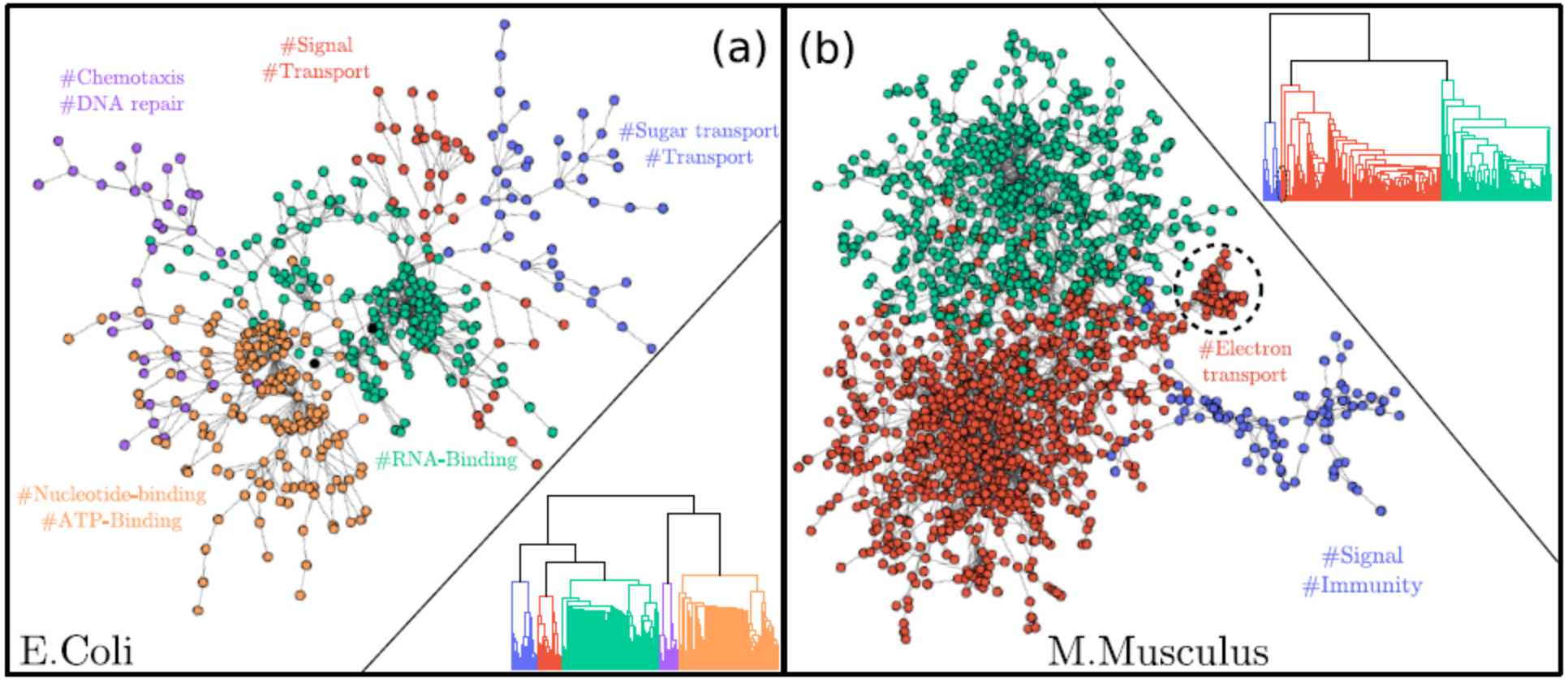

FIG. 6. Protein-protein interaction networks. (a) Modular structure of the E. coli PPI network for $\tau = 10$. The dendrogram illustrates the hierarchical clustering of the different nodes of the network. Different colors represent different communities and their corresponding main biological functions. (b) Modular structure of the M. Musculus PPI network for $\tau = 1$. The dendrogram illustrates the hierarchical clustering of the different nodes of the network. Different colors stand for different modules, as stated by the network dendrogram. Black nodes stand for metastable nodes. Note that instead of choosing the "optimal" network partition in terms of communication distances, we are now interested in the complex nested structure and modules of both organisms, giving rise to a rich structure with multiple overlapping communities. The different functionalities associated with each module are written in the same color as the nodes it contains. We stress the characterization of a small local module responsible for electron transport as a direct application of Ψ_ℓ (see black dashed circle). Note that here, we have integrated out the microscopic scales of both networks without going so far as to integrate out the Fiedler eigenvector, ensuring a proper analysis of the network mesoscopic modules.

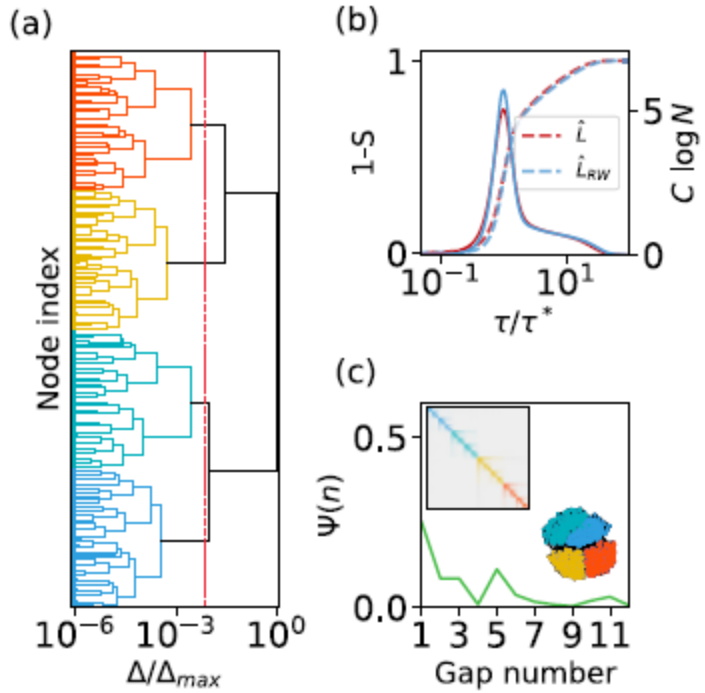

FIG. 9. Hierarchic modular network. (a) Normalized dendrogram for a HM-CP network using $\tau' = 1/\lambda_{\max}$. Red dashed line reflects the division of the network using the third gap of Ψ. Different communities are shaded in different colors. (b) Entropy parameter [dashed lines, $(1 - S)$] and specific heat (solid lines, C) versus the temporal resolution parameter of the network, τ. (c) Partition stability index (Ψ) versus gap number for $\tau = \tau'$. Note the high values of Ψ indicating the hierarchical structure of the network. Insets show the adjacency matrix and division into four communities of the network.

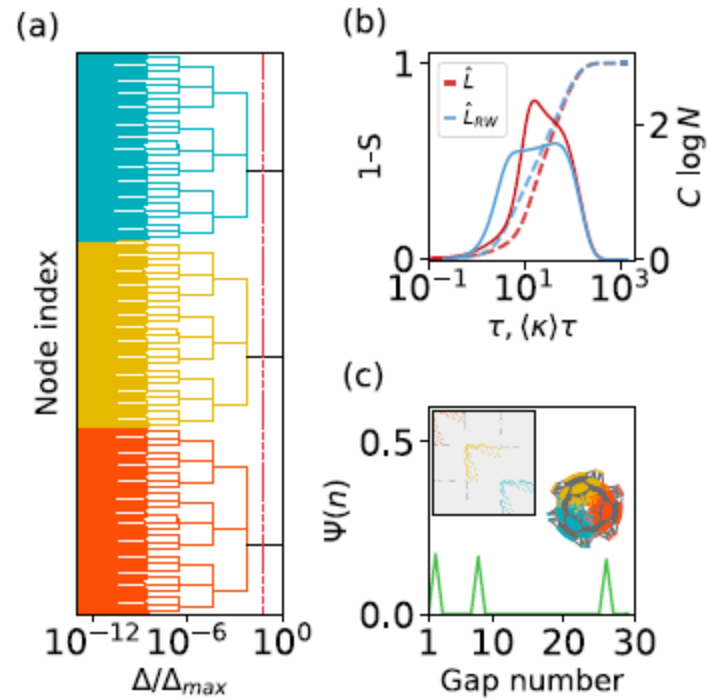

FIG. 10. Dorogovtsev-Goltsev-Mendes graph. (a) Normalized dendrogram for a DGM network using $\tau' = 1/\lambda_{\max}$. Red dashed line reflects the network division using the second gap of Ψ. Different communities are shaded in different colors. (b) Entropy parameter [dashed lines, $(1 - S)$] and specific heat (solid lines, C) versus the temporal resolution parameter of the network, τ. (c) Partition stability index (Ψ) versus gap number for $\tau = \tau'$. Note how peaks of Ψ are equally high, reflecting the precise hierarchical structure of the network. Insets show adjacency matrix and division into three communities of the network.

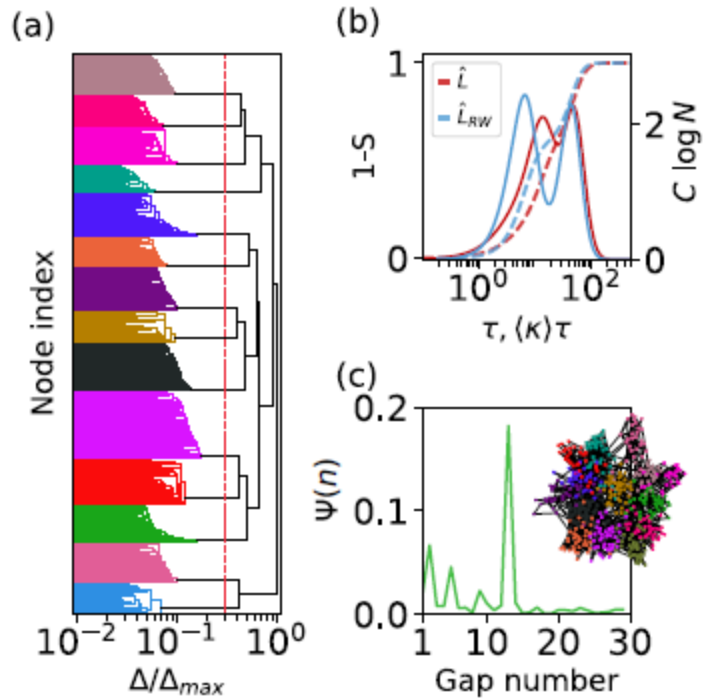

FIG. 12. Lancichinetti–Fortunato–Radicchi benchmark. (a) Normalized dendrogram for a LFR network using $\tau = 2$. Red dashed line reflects the network division using the optimal gap of Ψ. Different communities are shaded in different colors. (b) Entropy parameter [dashed lines, $(1 - S)$] and specific heat (solid lines, C) versus the temporal resolution parameter of the network, τ. (c) Partition stability index (Ψ) versus gap number for $\tau = 2$. Insets show network division into communities as set by the dendrogram.

Summary

- Finding multi-scale mesoscopic organization of communities is still a fundamental and open problem in complex network theory.
- Leveraging the **Laplacian Renormalization Group (LRG)**, we analyze information diffusion pathways across networks to shed light on this issue.

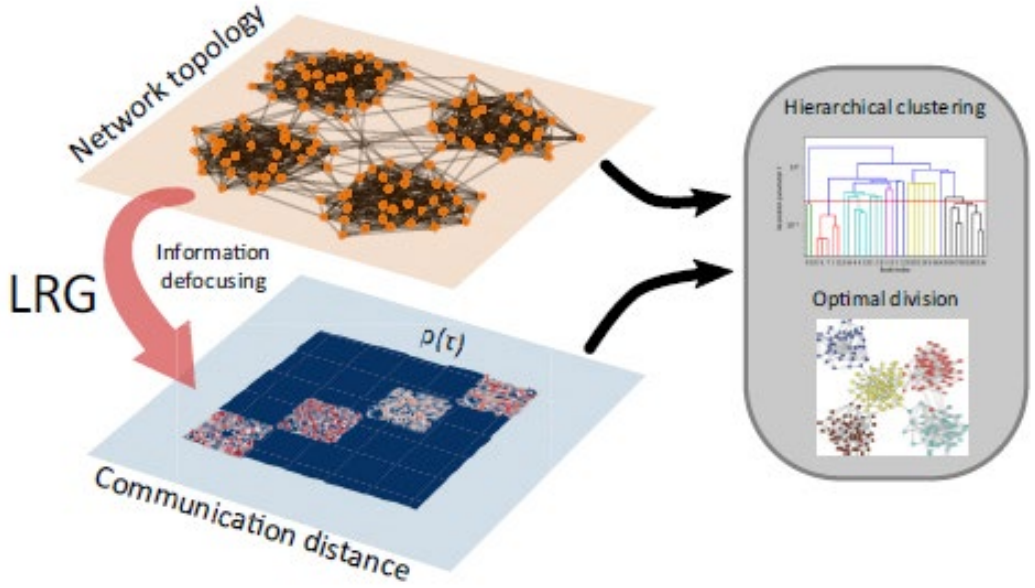

FIG. 1. Defining multiscale Kadanoff supernodes. *Communication distance* between nodes reflects the underlying hidden complex topology, capturing the internodes communicability and giving a natural merging of nodes at specific times τ. The LRG gives a natural interpretation of the network scales in terms of network eigenmodes, thereby enabling a deeper understanding of the mesoscopic properties of the network.